

Overpressure Estimation Using Combined Wireline data and Seismically-Generated Acoustic Impedance with Tectonic Evidences in a Niger Delta field.

¹Aigba, Paul I., ²Nwankwo, Cyril N. and ²Ekine, Anthony S.

⁽¹⁾ Department of Physics, Michael Okpara University of Agriculture, Umudike, Abia State, Nigeria.

⁽²⁾ Department of Physics, University of Port Harcourt, Port Harcourt, Nigeria.

Abstract: Overpressure issues in prospecting for hydrocarbon are critical, constituting an all-important input in drilling campaigns for economic and safety purposes. Estimation of overpressure using a combined approach is more reliable. Wireline log data and derived acoustic impedances (AI) of the seismic volume of this field were applied. The Eaton's modified model that converted compressional velocities to Vertical Effective Stresses were used to obtain the subsurface pore pressure (PP). The AI of a Prestack Depth Migration seismic volume was generated as its amplitude shows some tectonic issues. In well 1, 2132.8ms and 2268.6ms correspond to depths of between 2600m and 2800m on the log panel with a pore pressure gradient of 0.67psi/ft. From about 2700ms (above 3400m), AI decreased. Well 2 experienced a major drop in (AI) above 2000ms (2400m) and below 2300ms (2800m or 9240ft). Within this bracket, pore pressure gradient ranged between 0.66-0.74psi/ft with a peak of 0.74psi/ft at 2503m. Above 2500ms (3200m), seismic AI decreased to attain a pressure gradient of 0.74psi/ft. Well 1 is mildly overpressure while Well 2 is highly overpressure. Results show that this combined method is viable and recommended even at locations away from well control.

Keywords: tectonics, lithology, overpressure, acoustic impedance, checkshot.

I. Introduction

Deposition of sediments is accompanied by the expulsion of water. The increase in the overburden of the deposition is expected to translate to compensated-continuous liberation of water. However, when seals develop as a result of shale compaction, some formation water contained in it are trapped and prevented from draining. Disequilibrium compaction develops when the rate of fluid expulsion is dwarfed by the rate of deposition of sediment. This process may result to the development of abnormal fluid formation pressure. The Normal Compaction Trend (NCT) is a logarithmic plot that is of a linear trend maximally fitted measured data of transit time or velocity, density and resistivity which increases with depth as dewatering occur. Deviation from the normal compaction trend is assumed to represent a change in the porosity decline rate, which is associated with a change of pore pressure gradient up to a point of being abnormal. Compressional wave (P-wave) velocity is influenced by density, porosity, temperature, frequency, size of grain, gas saturation, effective stress and pore pressure.

Regional and local tectonics may be contributive to abnormal high pressure. Fluid formation pressures are affected by fault development, fractures, folding, compressions and plate tectonics caused by fault blocks down-dropping, salt diaper, movements of shale and many more. A downward or upward shift in fault could displace a fluid formation which may create a new passage for the migration of fluid resulting in an altered pressure. Alternatively, this may create an up-dip landmark for fluid isolation and conserve the formation pressure during a geodynamic process. This landmark may be generated by either the fault on its own or the juxtaposition of the non-permeable and permeable formation up-dip Sahay (1994). Formations with strong folds exhibit a pore volume decrease (as result of compression). Isolated blocks develop high fluid pressure (Chilingar et al, 2002).

The advent of regional and local tectonic activities pave way for cross flow along faults and compression loading and also do well to contribute to the secondary cause of overpressure. Local tectonic compression can also result to sediments that are overpressure (Badri et al., 2000). The correlation between abnormal formation pressure and propagation of cross fold joint in the Catskill delta of Central New York State is evident (Engelder and Oertel, 1985). Vertical effective stress no longer singly control compaction in tectonic climes as tectonic loading can lead to reduced vertical effective stress (Bower, 2002). Understanding the origin and evolution of overpressure is of the essence; in practice, the economic and safe drilling of wells are the results of overpressure comprehension (Gordon and Flemings, 1998). Overpressures in the Niger Delta region like other basins are established on disequilibrium compaction. However, secondary causes of overpressure are not unpopular as the delta displays a crisscross of both regional and local tectonics paving way to structural and stratigraphy issues amid other secondary factors may be active. The predicted top of overpressure is

mildly pressure (<0.71 psi/ft) at a depth of 10000ft True Vertical Depth (TVD) while high overpressure (>0.71 psi/ft) occurred at almost 13000ft in the area of interest of the X-field Onshore, Niger Delta. Observation is that this field's abnormal pressure seems to appreciate with depth in the direction of N-E (Ugwu and Nwankwo, 2013).

The use of wireline log data could be reliable in the estimation of overpressure along a well trajectory but may fail in predicting Geopressure in an entire field as various locations may experience different Geopressure regimes. Lower interval velocities obtained from seismic may be indications of overpressures as layers exhibit decreased porosities in shale, lower bulk densities, lower effective stresses and higher Poisson ratio. Porosity and pore pressure are some of the factors that mostly influence velocity change of P- wave. Such influences can infer abnormal pressure as either an expression of aquathermal expansion (Clay diagenesis or Catagenesis due to hydrocarbon maturation) or tectonic activities. Pore pressure is mainly a function of acoustic impedance. It can be deduced from acoustic impedance as well as from estimated velocity and density data since velocity depends on effective stress (Bowers, 1995). For all purposes, fluid pressure is mainly a function of acoustic impedance (Banik et al, 2013).

This study is targeted at estimating pore pressure in shale in an onshore Niger Delta field by applying a combined wireline log data and the seismically-generated acoustic impedance from a Prestack Depth Migration (PSDM) volume. The use of Measured Pore Pressure (MPP) from Repeat Formation Tester (RFT) is to standardize the estimated pore pressure obtained from normal compaction and Eaton's modified model at various depths with special attention on tectonic issues as influence on overpressure.

Regional Geology and Tectonics of the Niger Delta

The trenches and ridges of the Cretaceous fracture zones in the Atlantic Ocean control the tectonic regime of the West Coast of the equatorial Africa. The Cretaceous fracture zone is responsible for the division into basins including in Nigeria (Fig. 1). The Cretaceous Benue-Abakaliki trough represents a failed arm of a rift triple axis which relates to the opening of the South Atlantic. By Late Cretaceous, rifting reduced completely in the Niger Delta; although, it continued way into the Middle Cretaceous after commencing by the Late Jurassic (Lehner and De Reiter, 1977).

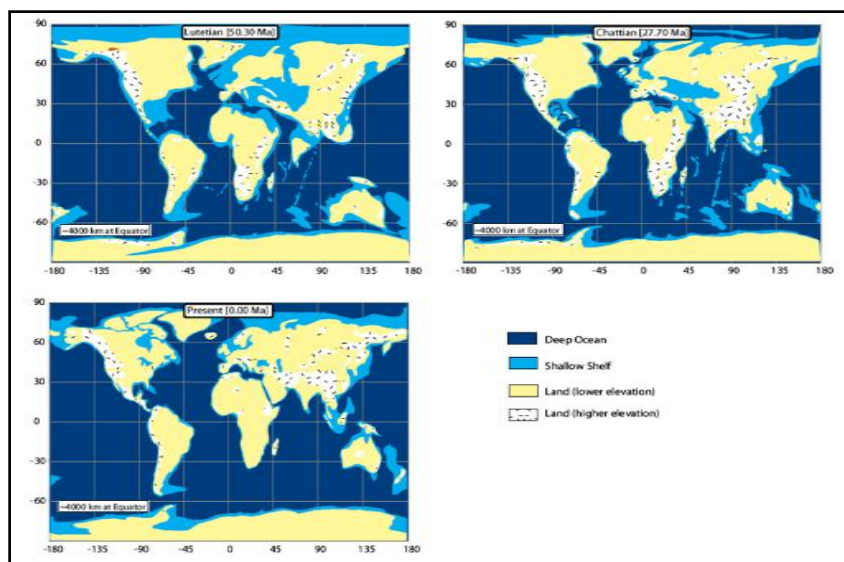


Fig. 1: The post Cretaceous or Cenozoic paleogeography of the Niger Delta as well as the relative position of the African and South American plates since the advent of rifting (After Turtle et al, 1999).

Gravity tectonics substituted rifting as a tectonic activity and was the basic process of deformation. Two processes initiated shale movement that caused deformation within the region (Kulke, 1995). Initially, the Agbada Formation's denser delta-front sand was responsible for shale diapirs which were formed by Akata Formation's poor compacted, overpressure adjoining delta clay. Finally, the non-lateral, basin direction non-support of Akata Formation's undercompacted delta-slope clays caused non-stability in gradient. In every depobelt of the region, gravity tectonic of complex structures such as diapirs of shale, anticlines of rollover, crest of growth fault which are collapsed, high gradient close flank faults, adjoining same features were completed before the sedimentation of the Benin Formation (Evamy et al., 1978; Xiao and Suppe, 1992). These faults register their strong impact on the Agbada Formation and straighten out as plane close to surface of Akata Formation (Fig. 2)

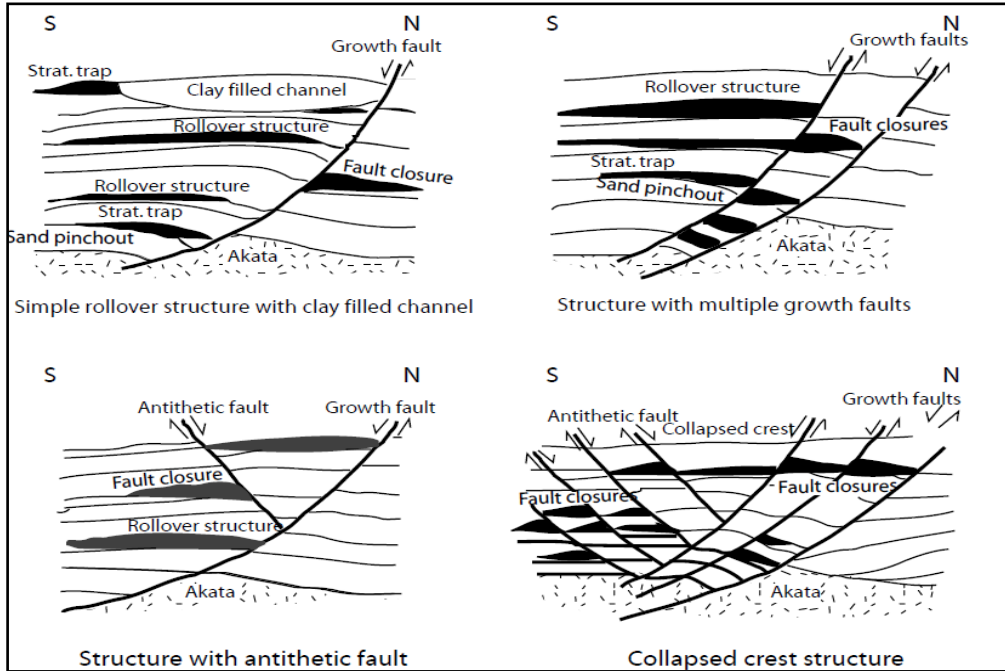


Fig.2: Types of traps associated with some Niger Delta field structures. After Doust and Omatsola (1990); Stacher (1995)

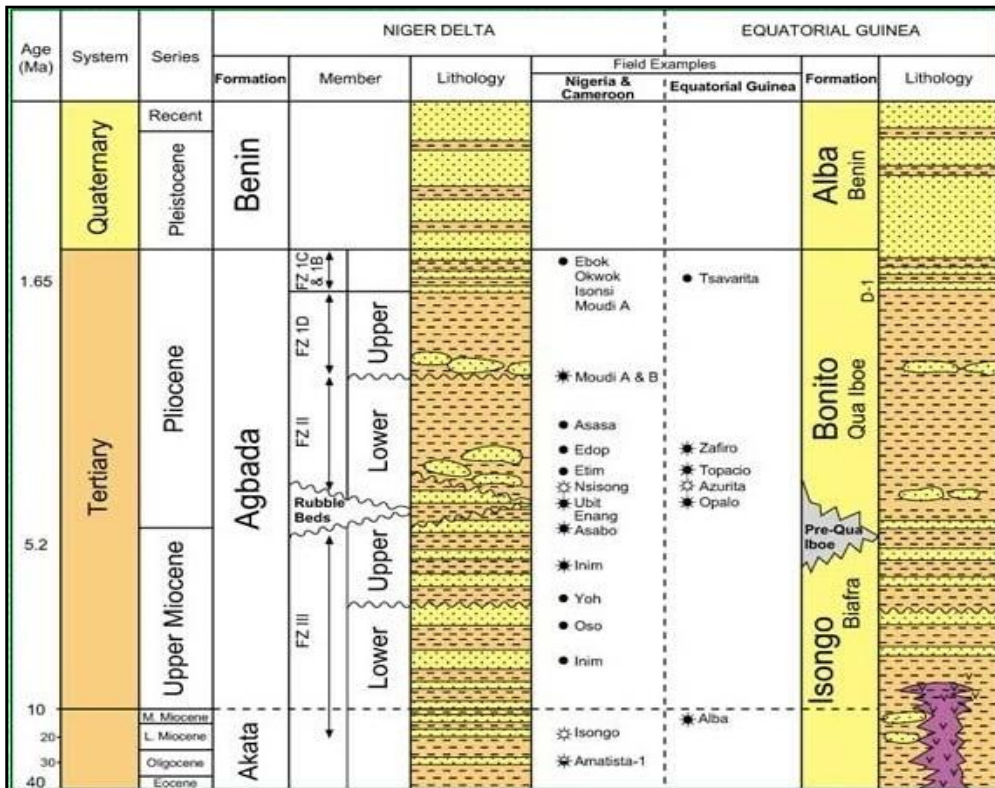


Fig. 3: The stratigraphy of the Niger Delta and Equatorial Guinea (After Kulke, 1995)

In the Niger Delta region, most fields have structural trap, however, stratigraphic traps exist as well (Fig.2). The syndeposition of deformation of the Agbada shale/sandstone intercalation sorting resulted in development of structural traps (Evamy et al, 1978; Stacher, 1995). Due to the sedimentation trend that characterizes the region, complex structure increases from North to South. The age of the Niger Delta ranges from Eocene of the overpressure shale Akata Formation to Recent age of sandstone Benin Formation through the Pliocene sandstone/shale alternating Agbada Formation (Fig. 3).

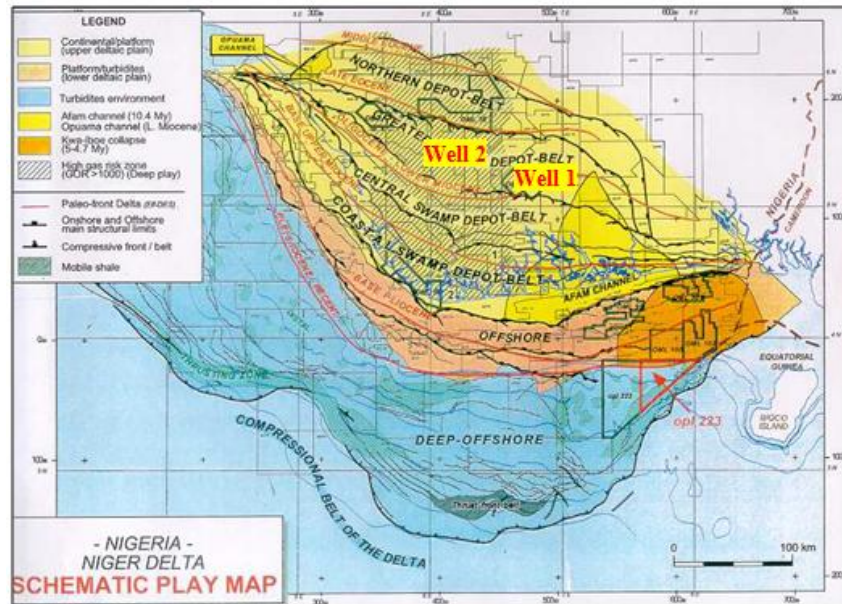


Fig. 4: Niger Delta depobelts showing the locations of the Wells in Greater Ughelli depobelt

II. Materials and Method

The data employed in this research work were Wireline data of gamma ray, sonic and density logs. Checkshot (TZ) data which converts time domain to depth were used. Drilling data of Repeat Formation Tester (RFT) for Measured Pore Pressure (MPP) and Prestack Depth Migration (PSDM) data were used to infer structural issues and acoustic impedances. The data were provided by Shell Petroleum Development Company (SPDC), Port Harcourt. The wells tagged 1 and 2 are both located at Greater Ughelli depobelt (Fig. 4). Well 1 has (Crossline, XL: 15628; Inline, IL: 7456) and Well 2 has (Crossline, XL:15372; Inline, IL:7818).

Generating Overburden Stress

The overburden stress (OBS) is the summation of the subsurface pressure at a given depth. This comprises of the effective stress due to the grain contacts and the pore pressure due to the fluid. The total stress is given by Terzaghi, (1943) as:

$$S = \sigma + p \quad 1$$

where S is the overburden stress, σ is the effective stress due to the matrix and p is the pore pressure.

The OBS is a derivative of density log either as a True Vertical Depth Subsea (TVDss) or True Vertical Depth Mudline (Zml) version. The TVDss has an inclusion of both seawater and atmospheric pressures while the latter do not contain any of the two.

The Normal Compaction Trend(NCT)

The transformation of vertical effective stress to pore pressure is given by Eaton (1975) as:

$$PP = OBS - (OBS - P_{hydro}) * (V_{obs}/V_{norm})^{n2}$$

where PP is pore pressure, OBS is Overburden stress, P_{hydro} is normal pressure at a given depth, V_n is the normal compressional velocity obtained from NCT at the defined depth V_{obs} is the observed compressional velocity at the same depth, and n is the Eaton's exponent which is age or basin location.

Acoustic Impedance (AI)

Acoustic impedance is defined as the product of the P-wave velocity and density of the layer in which it travels. It measures the contrast between two subsurface layers.

$$AI = \rho V$$

Seismic Trace at a particular depth (Amplitude) = Wavelet x RC

For two layers 1 and 2 concerned,

$$RC = \frac{\rho_2 V_2 - \rho_1 V_1}{\rho_2 V_2 + \rho_1 V_1} \quad 4$$

where AI is acoustic impedance ρ is density of a layer and V is the velocity of P- wave in it, RC is reflection coefficient (an interlayer factor).

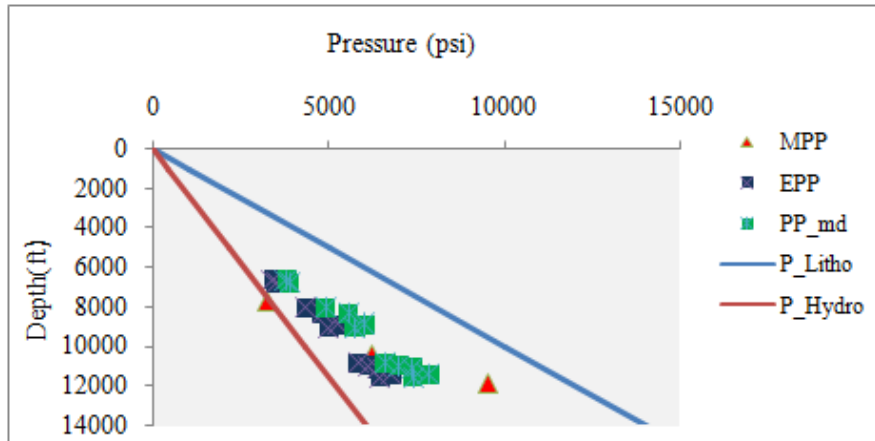


Fig. 5: The Pressure-Depth analysis of Well 1

The Pressure Depth plots in Figures 5 and 6 (see legends) consist of the hydrostatic pressure (P_Hydro) which symbolizes an approximate subsurface pressure baseline and the lithostatic pressure (peak subsurface pressure trend) at certain depths. The RFTs are represented by the MPPs while the Estimated Pore Pressures (EPPs) for normal compaction were generated using an Eaton index of 3. The plots represented as Eaton’s Pressure modified model (PP_md) rely on the strength of an index of 5.5. Take note of the trends followed by the two pressure estimates in both figures. PP_md did a better estimation than EPP in both cases and therefore adjudged to be more reliable input in the drilling programs of both wells.

The analysis of Figures 5 and 6 are represented in Tables 1 and 2 respectively; take cognizance of their PP_md. The tables relied on equations 1 and 2 to generate the Pore pressure and VES while a simple ratio of pressure versus depth was used in generating Pore Pressure gradient (PP_grad.). The red circled velocities in both tables are velocity reversals at various depths in the observed velocity (Vobs) columns.

Table 1: Pressure analysis of Well 1 using Eaton’s modified model

TVD(ft)	TVDss(m)	OBS(psi)	Vnorm	Vobs	PP(psi)	VES(psi)	PP_grad(psi/ft)
6616.04	2004.86	5926.24	2873.56	2689.66	3808.53	2117.72	0.58
6754.44	2046.80	6017.62	2873.56	2689.66	3878.04	2139.57	0.57
8027.81	2432.67	7495.55	3011.49	2781.61	4907.85	2587.70	0.61
8306.50	2517.12	7797.23	3011.49	2689.66	5549.12	2248.11	0.67
8913.63	2701.10	8109.06	3057.47	2689.66	6016.53	2092.53	0.67
9042.50	2740.15	10136.70	3057.47	2872.59	5732.50	4404.19	0.63
10830.00	3281.81	10264.30	3149.43	2919.54	6599.55	3664.77	0.61
10989.80	3330.24	10448.50	3195.40	2919.54	6994.50	3454.02	0.64
11100.50	3363.80	10605.20	3195.40	2873.56	7379.30	3225.86	0.66
11405.00	3456.07	10917.00	3195.40	2827.59	7873.07	3043.92	0.69
11566.00	3504.85	11072.20	3195.40	2919.54	7390.44	3681.74	0.64

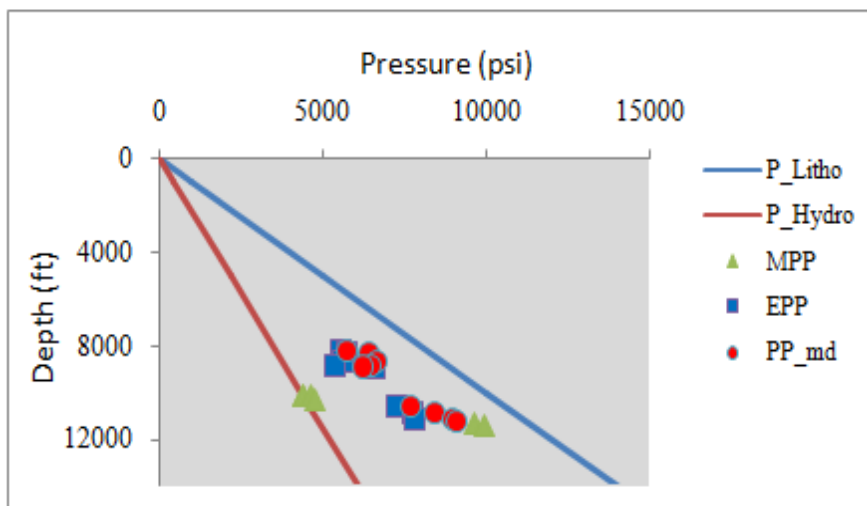


Fig.6 shows Pressure- Depth plot of well 2

Table 2: Pressure analysis of Well 2 using Eaton’s modified model

TVD(ft)	TVDss(m)	OBS(psi)	Vnorm	Vobs	PP(psi)	VES(psi)	PP_grad(psi/ft)
8179.94	2478.77	7402.73	3041.67	2708.33	5371.47	2031.26	0.66
8259.87	2502.99	7553.57	3041.67	2541.67	6077.89	1475.68	0.74
8632.90	2616.03	8007.53	3083.33	2708.33	5922.43	2085.10	0.69
8819.42	2672.55	8158.37	3083.33	2750.00	5853.26	2305.11	0.66
8979.30	2721.00	8158.37	3125.00	2750.00	6051.59	2106.78	0.67
10558.58	3199.57	9820.51	3291.67	2833.33	7526.08	2294.43	0.71
10867.63	3293.22	10122.18	3333.33	2791.67	8085.33	2036.85	0.74

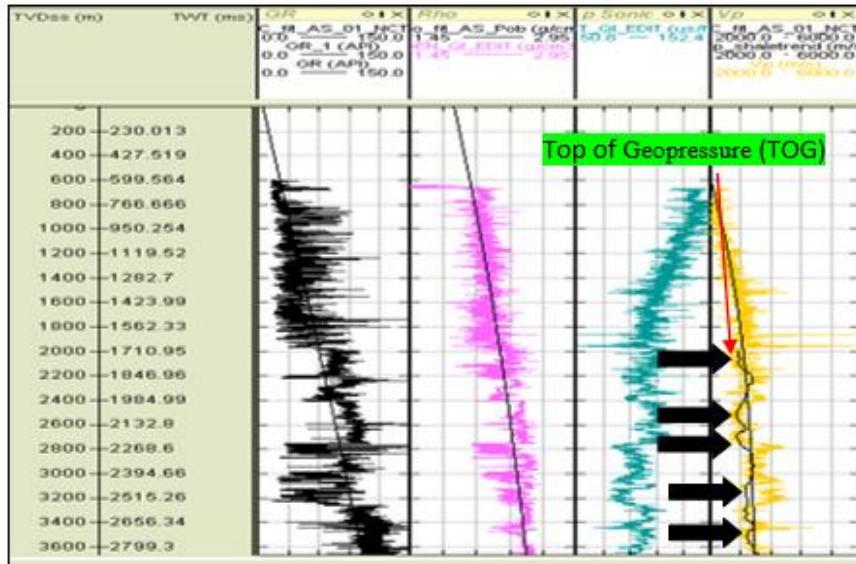


Fig. 8: Various important logs for Well 1

III. Discussion of results

Plotted Wireline log data of Well 1 consist of some of the key logs used for this research work. A correlation of the Gamma ray, density and the compressional wave velocity (V_p) logs shows that shale lithology as seen on the Gamma ray log corresponds to high density of formation at such depths and normally high P-wave velocity (Fig.8). In addition, a shale trend filter which delineated shale lithology with respect to shale thickness threshold was applied. As a deviation from the normal situation, as seen on the V_p track indicate sections exhibiting V_p reversals in shale. An appreciable velocity reversal indicates overpressure (Badri, et al, 2000). Results of these plots as deduced using Eaton’s models were presented in (Fig. 5 or Table 1). First incidence of velocity reversal was recorded at a depth range of 6616-7066ft (2004.5-2141.2m); this is the top of Geopressure (TOG) at a mild overpressure of 0.58psi/ft. The second tranche of velocity reversal started at a depth of 8027.81ft (2437.67m) to yield a vertical effective stress of 2587.7psi. The vertical effective stress of 2248.11psi at a depth of 8306.5ft(2517.12m) with an overpressure of 0.67psi/ft was the peak within this pressure pocket (Table 1). In instances where compartmentalization of rock allows pore pressures to counteract the vertical effective stress and undercompaction results, the outcome of this is to slow down the porosity decrease and rise in density and velocity (Chopra and Huffman, 2006).

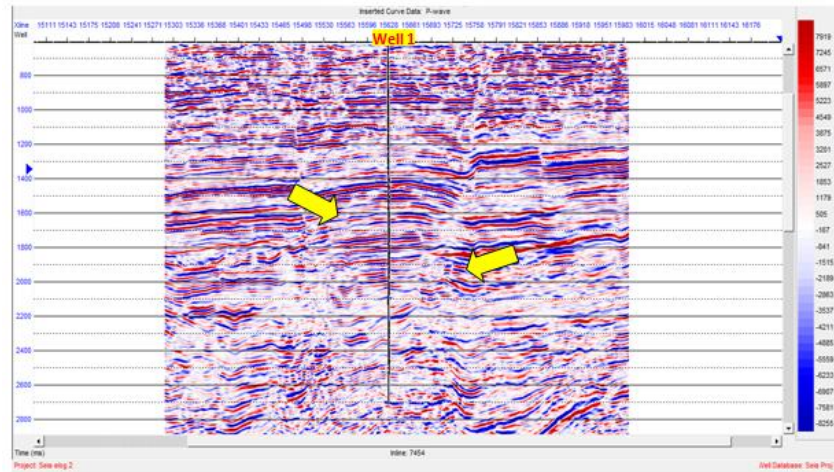


Fig.9: The location of well 1 in the field's seismic volume

The seismic volume in which well 1 is seated shows some fault line as arrowed to the left and some structural unconformities. The latter is visibly evident from 1800ms Two Way Time (TWT) and beyond (Fig. 9). In a Time-Depth (TZ) conversion of well to seismic tie, the depth of between 2000 and 2200m corresponds to time domain of between 1710.95 and 1846.8ms. This TWT coincides with the TOG (Fig. 8); the first noticeable pocket of meaningful shale trend and velocity reversal, although mild overpressure to a depth of 11880ft (3600m). In the Niger Delta, overpressures-driven by mega-structures and stratigraphy are common across the depobelts (Opara and Onuoha 2009).

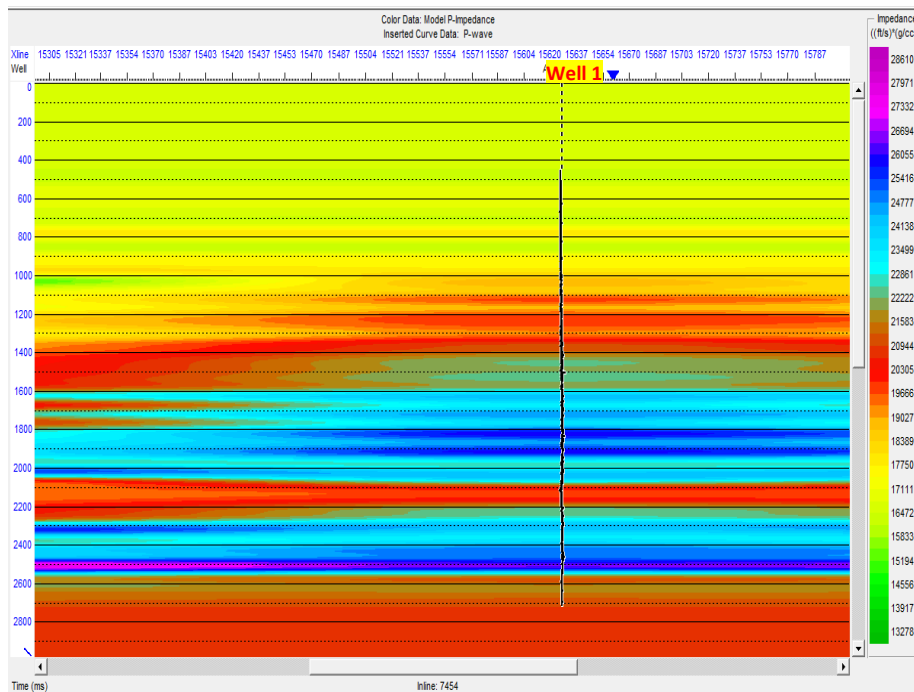


Fig.10: The Acoustic Impedance of the seismic volume through which Well 1 traverse

The acoustic impedance generated from the seismic volume shows the traverse of well 1 through various time domains. The product of P-wave velocity and density of each layer is indicated by the various colour intensities (see colour bar to the right of figure 10). A reduction in acoustic impedance is seen slightly above 2000ms to a little above 2200ms (Fig. 10). This translates to between 2132.8 and 2268.6ms (depth of between 2600 and 2800m or 8580 and 9240ft on the log panel) with a pore pressure gradient of 0.67psi/ft. Acoustic impedance increased thereafter and later dropped slightly at above 2600ms translating to a depth of between 3300m and 3400m. From about 2700ms (above 3400m depth) acoustic impedance decreased.

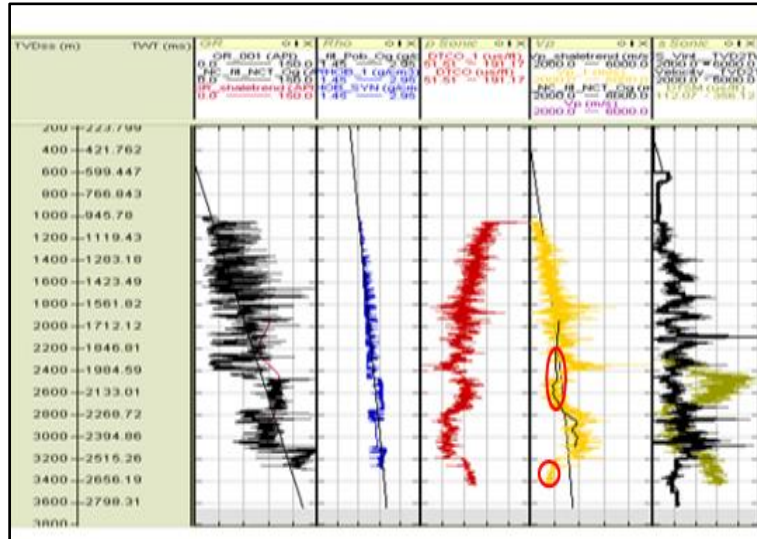


Fig. 11: Log plot for well 2

The results of the Eaton’s model which were obtained from wireline logs of Well 2 as plotted in figure 11 were presented in (Fig. 6 or Table 2). These show compressional velocity, Vp reversals with appreciable shale trend starting from 7260ft (2200m). However, the major reversal for a main shale lithology as indicated by the first red circle on the compressional log ranges between over 7920ft (2400m) to 9240ft (2800m) (fig. 11). Within this bracket, the maximum estimated pore pressure gradient is 0.74 psi/ft. At a depth of about 10890ft (3300m), the estimated pore pressure gradient increased to 0.74psi/ft from 0.71psi/ft at 10560ft (3200m). Wireline data for gamma ray log was not available for correlation beyond 3300m.

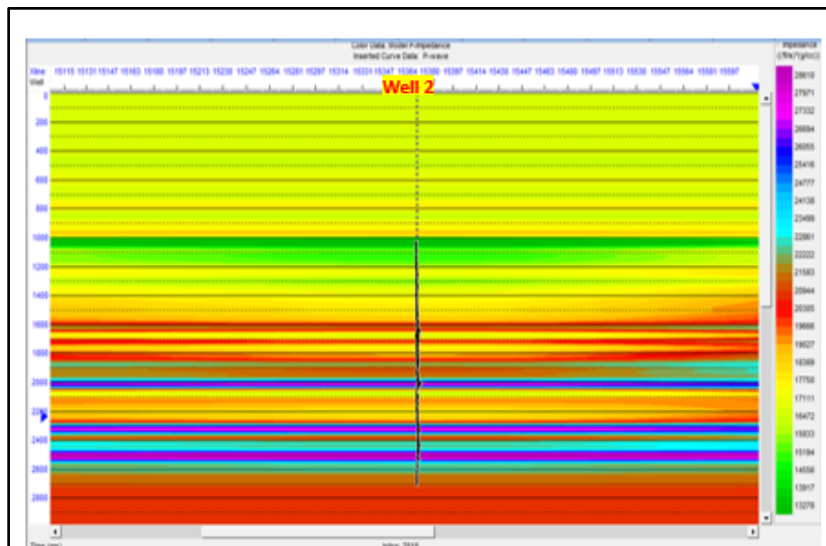


Fig.12 is the Acoustic Impedance of the seismic volume through which well 2 traverses

There is a reduction in acoustic impedanceslightly before 1700ms time domain (about 6600ft or 2000m depth); a departure from the earth model (fig. 12). A major drop in impedance was seen at above 2000ms (2400m or 7920ft) and below 2300ms (2800m or 9240ft). Within this bracket, pore pressure gradient ranged between 0.66-0.74psi/ft with a peak of 0.74psi/ft at 8260ft (2503m). Above 2500ms (10560ft or 3200m) on seismic volume, AI decreases for pressure gradient to be 0.74psi/ft at 10890ft or 3300m.

IV. Conclusion

From this study, it could be concluded that Well 1 is mildly overpressure (< 0.70psi/ft). There is an established trend of increase in overpressure from 6616.04ft True Vertical Depth (TVD) to 8913.63ft. The range of overpressure beyond this depth to 11566.00ft is 0.08psi/ft. Well 2 on the other hand is highly overpressure (>0.70psi/ft) at the stipulated depths. The increase in trend of overpressure was established from 8819.42ft

(TVD). There were agreements between the generated acoustic impedances from seismic volume and the different lithologies of both wells as seen from the wireline logs. Although, normal compaction is the primary cause of overpressure, it was visible from the seismic volume of the field that tectonics may have contributed to the overpressure issues that played out in the field under consideration. This is normal as the whole of Niger Delta is both structurally and stratigraphically controlled. However, it may not be ruled out that other secondary factors are contributive to the overpressure issues in this field. It is observed that the abnormal pressure of the field decreased in the S-W direction.

Acknowledgement

The authors are indeed grateful to Shell Petroleum Development Company (SPDC) for providing the data used for this research work. We are also indebted to Ikon science and Hampson Russell for providing the software used in analyzing the various data used.

References

- [1]. Badri, M. A., Sayers, C. M., Awad, R. and Graziano, A. (2000): A feasibility study for pore-pressure prediction using seismic velocities in the offshore Nile Delta, Egypt. *The Leading Edge*, Oct. 2000, pp 1103-1108.
- [2]. Banik, N., Koesoemadinata, A., Wagner, C., Inyang, C. and Bui, H. (2013): Pre-drill pore pressure prediction directly from seismically derived acoustic impedance, SEG 2013 Annual meeting, p 2905-2909.
- [3]. Bowers, G.L., (1995): Pore pressure estimation from velocity data: Accounting for overpressure mechanisms besides undercompaction; SPE Paper 27488, p.515-589.
- [4]. Bowers, G.L. (2002): Detecting high overpressure Applied Mechanics Technologies, Houston, Texas, U.S. *The leading edge*. Feb, 2002 pp 173-177.
- [5]. Chilingar, G.V., Fertl, W., Rieke, H. and Robertson Jr., J.O. (2002): Tectonics and overpressured formations. p. 191-208.
- [6]. Chopra, S. and Huffman, A. R. (2006): Velocity determination for pore-pressure prediction,
- [7]. Doust, H., and Omatsola, E., (1990): Niger Delta, *in*, Edwards, J. D., and Santogrossi, P.A., eds., *Divergent/passive Margin Basins*, AAPG Memoir 48: Tulsa, AAPG, p. 239-248.
- [8]. Eaton, B.A., (1975): The equation for Geopressure prediction from well logs, SPE.
- [9]. Evamy, B.D., Haremboure, J., Kamerling, P., Knaap, W.A., Molloy, F.A., and Rowlands, P.H., (1978): Hydrocarbon habitat of Tertiary Niger Delta: AAPG Bulletin, v. 62, p. 277-298.
- [10]. Gordon, D. S. and Flemings, P.B. (1998): Generation of overpressure and compaction-driven fluid flow in a Plio-Pleistocene growth-faulted basin, Eugene Island 330, offshore Louisiana Basin Research (1998) 10, p. 177-196.
- [11]. Kulke, H., (1995): Nigeria, *in*, Kulke, H., ed., *Regional Petroleum Geology of the World. Part II: Africa, America, Australia and Antarctica*: Berlin, GebrüderBorntraeger, p. 143-172.
- [12]. Lehner, P., and De Ruiter, P.A.C., (1977): Structural history of Atlantic Margin of Africa: AAPG Bulletin, v. 61, p. 961-981.
- [13]. Opara A.I. and Onuoha K.M. (2009): Overpressure and trap integrity studies in parts of the Onshore, Niger Delta Basin: implications for hydrocarbon exploitation and prospectivity, SPE J 240-242
- [14]. Sahay, B., (1994): *Petroleum Exploration and Exploitation Practices*. Allied Publishing. Ltd, New Delhi, p. 647.
- [15]. Stacher, P., (1995): Present understanding of the Niger Delta hydrocarbon habitat, *in*, Oti, M.N., and Postma, G., eds., *Geology of Deltas*: Rotterdam, A.A. Balkema, p. 257-267. TLE, Dec., 2006, pp. 1502-1504.
- [16]. Terzaghi, K., (1943): *Theoretical soil mechanics*, John Wiley and Sons Inc., New York
- [17]. Tuttle, M.L.W., Brownfield, M.E. and Charpentier, R. R., (1999): Tertiary Niger Delta (Akata-Agbada) Petroleum System (No. 701901), Niger Delta Province, Nigeria, Cameroon, and Equatorial Guinea, Africa. Open-File Report 99-50-H
- [18]. Ugwu, S. A. and Nwankwo, C. N. (2013): Integrated approach to geopressure detection in the X-field, Onshore Niger Delta. *J Petrol Explor Prod Technol* (2014) 4:DOI 10.1007/s13202-013-0088-4 p. 215-231.
- [19]. Xiao, H., and Suppe, J., 1992, Origin of rollover: AAPG Bulletin, v. 76, p. 509-529.